AIAA JOURNAL
Vol. 43, No. 5, May 2005

Luminescence Lifetime Response of Pressure-Sensitive Paint to a Pressure Transient

T. F. Drouillard II*
Colorado School of Mines, Golden, Colorado 80401
and
M. A. Linne†
Lund Institute of Technology, SE-221 00 Lund, Sweden

Pressure-sensitive paint (PSP) is used to acquire high-fidelity images of steady pressure distributions across surfaces. The PSP luminescence emission response to excitation light depends in a straightforward way on the oxygen concentration (hence air pressure) and the irradiance incident on the PSP lumiphores. Often, however, the phenomenon of interest is unsteady. During a rapid change in pressure, the oxygen concentration within a PSP layer varies with depth. Moreover, the excitation irradiance varies with depth as a result of attenuation, and this affects signal generation when the spatial distribution of oxygen is also changing. Prior studies have been reported on the transient response of PSP using the radiometric technique to detect pressure; we have extended the study by applying a luminescence lifetime technique. Oxygen concentration as a function of time and depth are obtained by solving the mass diffusion equation, with appropriate initial and boundary conditions. We develop a luminescence emission model that takes the spatially varying oxygen concentration and excitation absorption profile into account and relate pressure to the lifetime of the luminescence emission. Oxygen concentration is governed by mass diffusion of oxygen through a PSP layer during a rapid change in pressure, and the absorption of excitation light is governed by Beer's law. The significance of both the mass diffusivity and the optical depth of PSP are assessed. A numerical method was used to solve the mass diffusion equation that allows modeling of the oxygen concentration within the PSP given an arbitrary pressure function. We have used a double-image digital camera to acquire PSP emission lifetime data from several paint thicknesses during a rapid change in pressure. These data were compared to the results predicted by the model.

I. Introduction

IMAGING of surface air pressure using pressure-sensitive paint (PSP) is well established.[1–6] The photoreactive molecule in PSP luminesces when excited with an intense light source such as a laser. The resulting luminescence can then be detected with a charge-coupled-device (CCD) array. The excited-state lumiphore is selectively quenched by oxygen, and therefore the magnitude and lifetime of the luminescence signal depend on the partial pressure of oxygen in contact with the painted surface. The luminescence emission can therefore be related to the partial pressure of oxygen and thus air pressure. Demas et al.[1] have shown that the actual luminescence decay of PSP is most accurately modeled by the sum of several exponential terms, but that the single decay time constant that most closely fits the luminescence decay can be accurately related to pressure. The single-time-constant-based irradiance emission of PSP caused by an impulse of excitation light is given by

$$I(t) = I_0 e^{-t/\tau} \tag{1}$$

where I_0 (W/m^2) is the maximum luminescence at $t = 0$ and τ is the luminescence decay lifetime (μs).

The luminescence signal observed during PSP measurement relates to oxygen concentration (and ultimately to pressure when a pressure measurement is conducted) by the Stern–Volmer model for quenching of the irradiance. The radiometric and lifetime forms of the Stern–Volmer equation are[1]

$$I_A/I = 1 + K_{SV}[O_2] \tag{2}$$

$$\tau_A/\tau = 1 + K_{SV}[O_2] \tag{3}$$

respectively, where I_A and τ_A are the time-integrated irradiance and the decay time constant in absence of a quenching molecule (in this case oxygen), I and τ are the time-integrated irradiance and decay time constant of the luminescence in the presence of oxygen, and K_{SV} (units of inverse oxygen concentration, e.g., m^3/mole O_2) is the Stern–Volmer coefficient. For pressure measurements a variation in the partial pressure (kPa or torr) of oxygen can be related to pressure under steady-state pressure conditions. In this case the right-hand sides of Eqs. (2) and (3) are expressed as $1 + kP$, where P (torr) is the air pressure and k (torr^{-1}) is a coefficient representing a modified form of the Stern–Volmer constant that converts the partial pressure of oxygen to atmospheric pressure.

In the radiometric technique, one applies an excitation pulse and measures the time-integrated luminescence intensity throughout the luminescence decay under a static, known pressure condition. This wind-off measurement is used as an irradiance reference rather than acquiring I_A under vacuum conditions, which in general is experimentally impractical. Pressure is then measured by applying an excitation pulse during wind-on conditions and measuring the time-integrated luminescence emission. This technique is therefore limited to measurements of pressures that are time invariant over the duration of luminescence decay because any change in pressure during acquisition of the time-integrated signal would corrupt the measurement.

In the lifetime technique, one applies an excitation pulse and measures the time-resolved luminescence decay, and from this decay curve one extracts the luminescence lifetime. Multidimensional (surface) lifetime measurements have been obtained previously by rastering single-point excitation and detection over a test object,[7,8] by exciting the test object with a periodic illumination source and detecting the phase delay of the luminescence emission relative

Received 23 January 2004; revision received 25 June 2004; accepted for publication 11 November 2004.

*Graduate Research Assistant, Division of Engineering; tdrouill@ball.com.
†Professor, Department of Combustion Physics.

to the excitation with a phase-sensitive camera (where the decay time constant is then calculated from the phase angle and excitation frequency; a technique developed for the detection of fluorescence lifetime measurements in biochemical analyses),[9–11] and by double-image techniques.[12] Of these, the double-image approach offers the advantage that a spatial distribution of pressure is obtained from one excitation pulse. It has also been shown that the two-gate technique offers pressure sensitivity superior to that of phase detection methods.[11]

Recent accuracy assessments of the lifetime measurement technique,[10,11,13] based on earlier error analyses of Oglesby et al.[14] and Sajben,[15] quantitatively show that radiometric techniques show less error in the Stern–Volmer equation at low pressure than lifetime techniques; however, the error introduced by wind-off supercede the uncertainty in the Stern–Volmer equation. It has also been shown that the sensitivity of the lifetime technique significantly exceeds the sensitivity of the radiometric technique.[11]

Most of these results have been acquired under steady pressure and temperature conditions. A number of flowfields of interest, however, involve pressure transients (e.g., transitional flows). If the pressure transient is fast relative to the total response time of the paint, these steady flow approaches are not necessarily accurate. During a rapid change in pressure, the oxygen concentration within a PSP layer varies with depth. Moreover, the incident irradiance varies with depth caused by attenuation, and this can affect signal generation when the spatial distribution of oxygen is also changing. Some research has been performed on the transient response of PSP and the effects of PSP thickness.[16–18] We have performed a somewhat more detailed study, however, in order to evaluate what phenomena must be included when transient data are analyzed. In what follows, we review the existing literature on the transient response of PSP, describe the development of a more detailed model that requires numerical solution, describe experiments performed to evaluate the model, and then draw conclusions on what kind of model is necessary for accurate analysis of PSP response to pressure transients.

II. Background

There have been several investigations into the response of PSP to pressure transients. Baron et al.[19] stated that the response of PSP to a rapid change in pressure is governed by the oxygen diffusion rate through the binder; PSP response depends on paint thickness and oxygen diffusivity of the binder material. They conducted experiments that demonstrated the use of different binders. For these experiments, a PSP sample, under excitation by steady-state short-wavelength illumination, was subjected to a rapid change in pressure. The spatially integrated emission response was acquired with a photomultiplier tube. Response times of several binder types were compared.

Carroll et al. modeled PSP emission response to steady-state luminescence excitation during a step increase in pressure by solving the mass diffusion equation with a positive-step driving function.[16] They used a laboratory setup similar to that used by Baron et al. and tested three lumiphore/binder configurations of varied thickness to verify their model.

Winslow et al. modeled PSP emission during steady-state luminescence excitation and a sinusoidally varying pressure field.[20] Their model included a solution of the mass diffusion equation with a sinusoidal driving function. They conducted experiments using an apparatus similar to those used by Baron et al. and Carroll et al. with oscillating pressure. Analyses were performed in the frequency domain. Their conclusions were that the physical characteristics of a PSP (binder diffusivity, thickness, etc.) determine its response to changes in pressure and that the response time of a PSP layer to a change in pressure is inversely proportional to the square of the thickness. The response time cited by Winslow et al. is the time constant for oxygen concentration in a layer of PSP to reach equilibrium with atmospheric partial pressure of oxygen following a pressure step. In the experiments reported here, PSP samples of varied thickness were exposed to pressure changes that occurred over several hundred milliseconds; thus, the change in pressure was on the temporal order of the expected response time of a PSP layer.

In a recent paper, Winslow and coworkers developed an irradiance model by recasting the mass diffusion equation (along with the initial and boundary conditions) in terms of PSP emission response to steady-state excitation.[21] In that study, a luminescence emission model based upon the depth profile of oxygen concentration was derived and integrated to give the total irradiance; absorption and scattering of excitation light and PSP luminescence was not considered. In each of these studies, the radiometric form of the Stern–Volmer relation was applied to integrated irradiance measurements.

In a paper closely related to the present work, Schairer modeled the effects of PSP thickness under transient pressure conditions using the radiometric technique.[18] Schairer developed an analytical model of the total luminescence emission of PSP as the emission per unit depth, integrated over the paint thickness. The emission was related first to sinusoidally varying pressure by the radiometric form of the Stern–Volmer equation, and the perceived pressure was related to actual pressure by an amplitude ratio and a phase difference. The sinusoidal pressure was then generalized by including higher-order harmonic terms. Schairer showed that as pressure frequency increases increased PSP thickness causes measurement distortions as a result of relatively slow diffusion of oxygen through the PSP layer.

In the present work, the lifetime PSP technique, a numerical solution to the mass diffusion equation, and Beer's law for irradiance attenuation in an absorbing and scattering medium are used to develop an irradiance impulse response model under dynamic pressure conditions. Laboratory results are presented in which a scientific-grade dual-image interline transfer CCD (ITCCD) camera was used to acquire luminescence lifetime measurements of PSP during a rapid pressure change, as described previously.[12] Several sample thicknesses of PSP were prepared on an oxygen-impermeable silicon substrate; thicknesses were measured, and measured lifetime responses were compared to predicted results.

III. Theory

A. Lifetime PSP Technique

The lifetime PSP technique presented here is based largely on the work of Goss et al.[11] Following excitation by an impulse of light, PSP luminescence decays exponentially from an initial irradiance I_0 to zero, given by Eq. (1) and shown in Fig. 1. Two camera exposures, denoted by m_1 and m_2 in Fig. 1, are captured during the luminescence decay. Here, m_1 corresponds to an acquisition interval beginning at time t_0 and ending at time t_1. Similarly, m_2 corresponds to an image acquisition interval beginning at time t_1 and ending at time t_f. The duration of the second image is sufficiently long that the luminescence emission is negligible at the conclusion of the exposure.

Expressions for m_1 and m_2 calculated as integrals of the exponential decay function are

$$m_1 = \int_{t_0}^{t_1} I_0 e^{-t/\tau}\,\mathrm{d}t = I_0\tau(e^{-t_0/\tau} - e^{-t_1/\tau}) \tag{4}$$

$$m_2 = \int_{t_1}^{t_f} I_0 e^{-t/\tau}\,\mathrm{d}t = I_0\tau e^{-t_1/\tau} \tag{5}$$

where I_0 represents the luminescence irradiance at $t = 0$ and t_f is sufficiently larger than τ such that $e^{-t_f/\tau} \approx 0$. The dimensionless

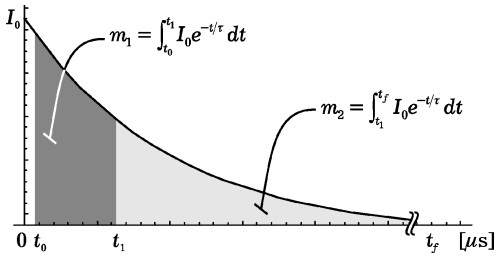

Fig. 1 Double-image acquisition of exponential luminescence decay.

ratio m_1/m_2 is

$$m_1/m_2 = e^{(t_1 - t_0)/\tau} - 1 \tag{6}$$

Equation (6) can be explicitly solved for τ:

$$\tau = \frac{t_1 - t_0}{\ell_n(1 + m_1/m_2)} \tag{7}$$

If t_0 and t_1 are known and m_1 and m_2 are measured, the decay time constant τ can be calculated from Eq. (7) and in turn used to calculate pressure by the lifetime Stern–Volmer relation.

B. Light Attenuation by PSP

The luminescence emission of PSP is affected by absorption and scattering of excitation light by PSP lumiphores. Here transmissivity of PSP is discussed, and the effect of absorption and scattering is discussed in later sections. When a layer of PSP is exposed to excitation light, the irradiance decreases exponentially with depth into the paint layer according to Beer's law[22]:

$$I(z, t) = I(0, t)e^{-\kappa_\nu z} \tag{8}$$

where $1/\kappa_\nu$ is the optical depth of the PSP, for green ($\lambda = 532$ nm) light in this case. Optical depth is the distance into the medium at which the excitation irradiance is $1/e$ ($\sim$36.8%) that of the unattenuated light.

Although the PSP emission (red) light also undergoes attenuation, it is negligible on the scale of the excitation absorption.[18,21] In our own work, when measured attenuation of red light was incorporated with reasonable values for luminescence yield the PSP emission attenuation profile had little effect on the outcome, which was dominated by the attenuation of green light and by the O_2 concentration profile. The model is simply more sensitive to 532-nm absorption and to oxygen concentration profiles, owing to the low values for luminescence yield, and therefore red attenuation was neglected in this model.

C. Irradiance Modeling Under Dynamic Pressure Conditions

Winslow et al. developed a model for luminescence emission from a layer of PSP under dynamic pressure conditions by establishing a luminescence density (irradiance per unit depth) expression $J(z, t)$ and integrating over the thickness of the PSP layer to give the total luminescence emission $I(t)$ (Ref. 21). Here we take a similar approach, incorporating Beer's law to account for absorption at a depth z.

Under dynamic pressure conditions, the oxygen concentration n within a layer of PSP varies with depth and time: $n = n(z, t)$. For this discussion, the temporal variation of $n(z, t)$ as a result of rapidly changing pressure is on the order of hundreds of milliseconds while PSP luminescence decay is on the order tens of microseconds. Therefore, the oxygen concentration immediately following a luminescence excitation pulse at $t = t_p$ is $n_p(z) = n(z, t_p)$, and it varies negligibly during the duration of PSP luminescence emission. This is significant here because the luminescence response of PSP depends on the oxygen concentration within the PSP layer. Measurements during a rapid pressure change (i.e., during a rapid change in the oxygen concentration within a PSP layer) must be sufficiently fast that the oxygen concentration (and therefore the luminescence response) does not change significantly from the beginning of the luminescence measurement to the end of it.

Winslow et al. define irradiance per unit depth $J(z, t)$ that, when integrated over z, gives the total irradiance emission from the PSP, that is,

$$I(t) = \int_z J(z, t)\,\mathrm{d}z \approx I_0 e^{-t/\tau} \tag{9}$$

$J(z, t)$ varies with depth as a function of oxygen concentration $n_p(z)$.

Integrating $J(z, t)$ over a thin "slice" Δz within the PSP layer gives the irradiance at a depth z. The irradiance from a thin layer at a depth z resulting from an excitation impulse is the luminescence decay function caused by an oxygen concentration $n_p(z)$. The excitation pulse incident on a layer at a depth z is scaled according to Beer's law. The irradiance from a thin layer at a depth z is

$$\Delta z J(z, t) = I_z e^{-t/\tau_z} \tag{10}$$

where I_z and τ_z are the emission irradiance and lifetime caused by the oxygen concentration $n_p(z)$, given by the Stern–Volmer equations

$$I_z = \frac{I_A e^{-\kappa_\nu z}}{1 + K_{SV} n_p(z)}, \qquad \tau_z = \frac{\tau_A}{1 + K_{SV} n_p(z)} \tag{11}$$

Note that I_z is scaled by an attenuation term $e^{-\kappa_\nu z}$ satisfying Beer's law. The complete model for the decaying luminescence emission caused by an excitation pulse at t_p is

$$I(t) = \int_0^\theta \frac{I_A e^{-\kappa_\nu z}}{1 + K_{SV} n_p(z)} \exp\left\{-[1 + K_{SV} n_p(z)]\frac{t}{\tau_A}\right\} \mathrm{d}z \approx I_0 e^{-t/\tau} \tag{12}$$

where θ is the thickness of the PSP layer.

D. Mass Diffusion Equation and Finite Difference Solution

The quasi-instantaneous oxygen concentration $n_p(z)$ appearing in Eq. (12) is modeled by mass diffusion of oxygen through the permeable PSP during a rapid change in pressure. The mass diffusion equation in one spatial dimension z is

$$\frac{\partial^2 n}{\partial z^2} = \frac{1}{D_m}\frac{\partial n}{\partial t} \tag{13}$$

where $n(z, t)$ is the oxygen concentration within the PSP layer at a depth z and time t, and D_m is the mass diffusivity of the PSP ($D_m = 1000\ \mu\mathrm{m}^2/\mathrm{s}$ is used here; this is a typical value[18]). The PSP boundaries are $z = 0$ at the air/PSP interface, and $z = \theta$ is the thickness of the PSP layer. The oxygen concentration at the PSP/atmosphere interface is given by Henry's law

$$n(0, t) = \sigma_H P(t) \tag{14}$$

where σ_H is Henry's constant that relates oxygen concentration to pressure. Because σ_H varies with temperature, constant temperature was maintained.

The silicon substrate to which PSP was applied is not oxygen permeable, the boundary condition at the PSP/substrate interface is therefore given by Fick's law

$$\left.\frac{\partial n}{\partial z}\right|_{\theta, t} = 0 \tag{15}$$

The initial condition

$$n(z, 0) = 0 \tag{16}$$

indicates that the PSP was held at vacuum sufficiently long that any significant concentration of oxygen diffused out of the sample.

A numerical solution to the mass diffusion equation along with the specified initial and boundary conditions was implemented with a finite difference technique to give $n(z, t)$ (Ref. 23). The instantaneous oxygen concentration $n_p(z) = n(z, t_p)$ obtained by solving the mass diffusion equation was used in Eq. (12) to obtain a predicted emission irradiance function $I(t) \approx I_0 e^{-t/\tau}$. The lifetime τ of the modeled emission irradiance function was calculated for comparison to experimental results.

To calculate a numerical solution, several results were required. In Eq. (12), $1/\kappa_\nu$ was determined by a transmission experiment, and $n_p(z)$ was determined over a range of discrete depths z_i. The vacuum ($P = 0.12$ torr) lifetime τ_A was measured as 60.3 μs. The Stern–Volmer constant K_{SV} was calculated from static-pressure lifetimes at vacuum and atmosphere ($\tau = 10.6\ \mu$s when $P = 692$ torr in our case). The straight-line Stern–Volmer constant for relative

concentrations comes from solving Eq. (3) for K_{SV}, which gives $K_{SV} = 4.70$.

The integral in Eq. (12) was calculated as a sum over Δz, sampled 30 times over a 300-μs interval and fit to a single-exponential function by the Levenberg–Marquardt nonlinear fitting algorithm. Luminescence decay time was then tabulated against t_p and compared to lifetime measurements.

IV. Laboratory Apparatus

Laboratory experiments were conducted to verify the model. A PSP sample at vacuum ($P \sim 0.12$ torr) was exposed to a rapidly increasing pressure function $P(t)$ that started at $t = 0$ and reached atmospheric pressure ($P = 692$ torr) at $t \sim 250$ ms. Pressure was measured at discrete times during the pressure change using the luminescence lifetime technique and simultaneously with a pressure transducer for comparison.

A. Sample Preparation and the Pressure Chamber

A sample was prepared by applying five thicknesses of PSP to a silicon wafer ($\sim 20 \times 25$ mm). The PSP (Uni-FIB from ISSI) consisted of a fluorinated platinum porphyrin [Pt(TfPP)] lumiphore in a fluoroacrylic copolymer (FIB) base and was applied with an airbrush (Badger No. 150, fine-tip). PSP sample thicknesses were measured using a profilometer.

Figure 2 shows a drawing of the pressure apparatus and sample holder that was used. The sample holder was constructed from copper and included a water-circulation tube for maintaining the PSP sample at a constant temperature of 10°C. Pressure inside the vessel was reduced to 200 mtorr by a vacuum pump, then impulsively filled to atmospheric pressure by closing a valve on the vacuum line and triggering a solenoid valve that opened the vessel.

B. Chamber Pressure Measurements

Static-pressure measurements were made using a barratron with a range of 10–1000 torr and a thermocouple gauge with a range of 0.01–1 torr. Chamber pressure measured as a function of time during the filling procedure was detected by a piezoelectric pressure transducer and recorded on a digital oscilloscope. The trigger signal (which coincided with an excitation pulse) that initiated image acquisition was also recorded on the digital oscilloscope to resolve the time of the excitation relative to the pressure ramp. Each digitized pressure signal was recorded as a list of 2500 (time, voltage) data points. Transducer voltage data points were converted to pressure data points by subtracting a 50-s exponential decay background function and scaling by a calibration factor (as suggested by the pressure transducer manufacturer). The equation applied to each voltage value v_i obtained at a time t_i to obtain a corresponding pressure value P_i was

$$P_i = \frac{51.715 \text{ torr}}{10 \text{ mV}}[v_i + 1.434(1 - e^{-t_i/50})] \tag{17}$$

where the 51.715 torr/10 mV ratio and 50-s time constant are parameters cited by the transducer manufacturer, and the factor of 1.434 was determined empirically based on initial and final static-pressure measurements made with a thermocouple gauge and barratron, respectively. Pressure vs time data are plotted in Fig. 3. Fifty-seven repetitions of the pressure transient shown in Fig. 3 were compared to verify repeatability of the pressure transient. The standard deviation of transducer-measured pressure as it varied with time is plotted in Fig. 4.

Pressure and time rate of change of pressure (dP/dt) at the moment of the excitation pulse were calculated by fitting a fourth-order polynomial to a subset of 250 (t, P) data points; the center point used to define the limits of each subset was determined by the time of the excitation pulse.

C. Optical and Imaging Systems

The vacuum vessel was fitted with viewports on two orthogonal sides for transverse optical access. Excitation light entered the vacuum vessel through one viewport and luminescence was collected through the other, as shown in Fig. 5. The sample was illuminated by green ($\lambda = 532$ nm) light pulses from a frequency-doubled

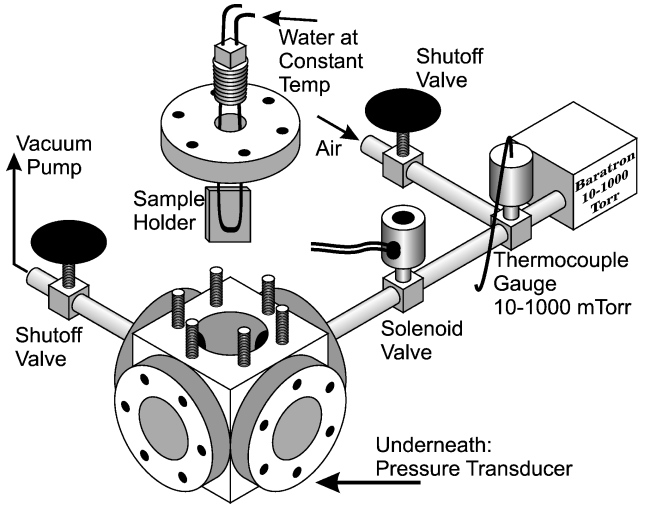

Fig. 2 Vacuum system.

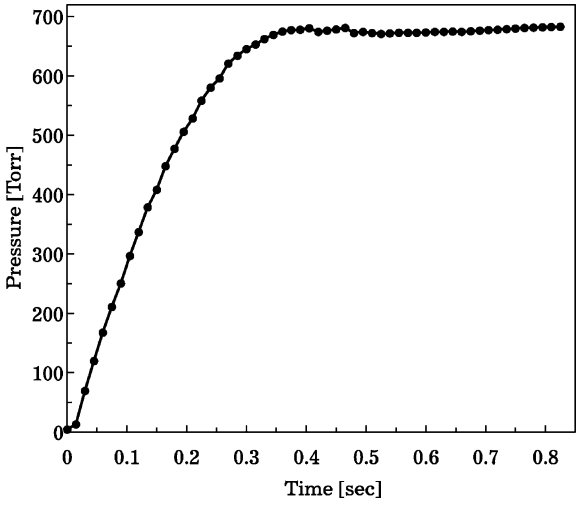

Fig. 3 Transient pressure function measured by the pressure transducer.

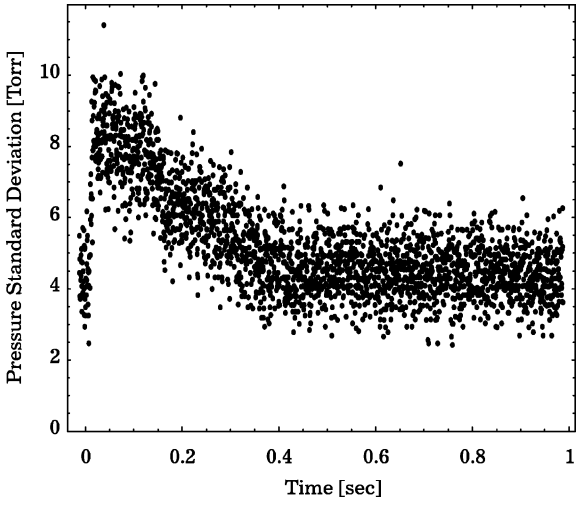

Fig. 4 Standard deviation of transducer-measured pressure during the transient pressure event.

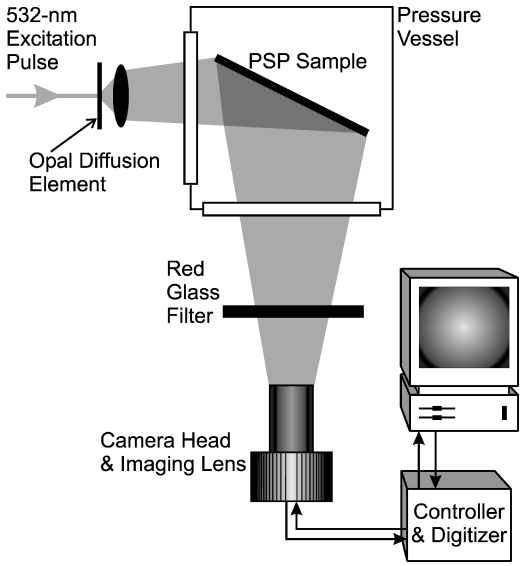

Fig. 5 Excitation and imaging apparatus.

Q-switched Nd:YAG laser. The laser was operated at a 10-Hz repetition rate, the pulse duration was 9 ns, and the energy delivered to the sample was ~140 μJ/pulse.

Luminescence emission was collected using a scientific-grade ITCCD double-image feature camera (Micro-MAX by Roper Scientific/Princeton Instruments, Inc.). The camera was fitted with a 105-mm Nikon imaging lens. A long-pass filter (cutoff wavelength ~600 nm) in front of the camera lens reduced scattered light entering the camera.

The camera's dual-image timing mode (described in detail by Drouillard et al.[12]) was used to acquire two sequential exposures following an excitation pulse. The first exposure was 10 μs and began ~2 μs after the excitation pulse. The second exposure was 8.01 ms and began immediately after the first image was acquired.

V. Results and Discussion

A. PSP Transmissivity

Transmission of 532-nm light at various PSP thicknesses was acquired by applying several thicknesses of PSP to microscope slides (12 thickness samples ranging from ~3 to ~47 μm). Thicknesses were measured using a profilometer (model P-10 by Tencor Instruments) to acquire six thickness profiles across each region of uniform paint thickness. Thickness and roughness were calculated as the average and standard deviation across a region. A spectrophotometer (Cary 5G by Varian Optical Spectroscopy Instruments) was used to measure percent transmission of monochromatic light (integer wavelengths from 300 to 800 nm) through 11.4 × 18.5-mm surface regions of uniform thickness. Percent-transmission spectra of PSP samples with mean thicknesses of 2.99 and 18.7 μm are plotted in Fig. 6.

A Levenberg–Marquardt algorithm was used to fit transmission-vs-thickness data (transmission of 532-nm light) to Eq. (8). The transmission data and fitted curve are plotted in Fig. 7. The fit produced $1/\kappa_\nu = 6.48$ μm for 532-nm light. Horizontal bars denote the roughness measurement. The vertical error component of Fig. 7 is the uncertainty of the spectrophotometer measurement. According to the manufacturer specifications, the uncertainty in the transmission measurement is <0.0004 (0.04%), wavelength uncertainty is ±0.1 nm, and positional reproducibility (causing changes in reflectivity) contributes <1%.

B. Thickness Measurements

Thicknesses of samples that were prepared for the rapid pressure experiment were measured with the profilometer. Figures 8–12 show profilometer data acquired in each of five thickness regions. Mean thickness values are shown as dashed lines. The profilometer sampled at 10-μm intervals; the profile in Fig. 8 for example consists of 280 points sampled over 2.8 mm. Seven profiles were acquired from each thickness region.

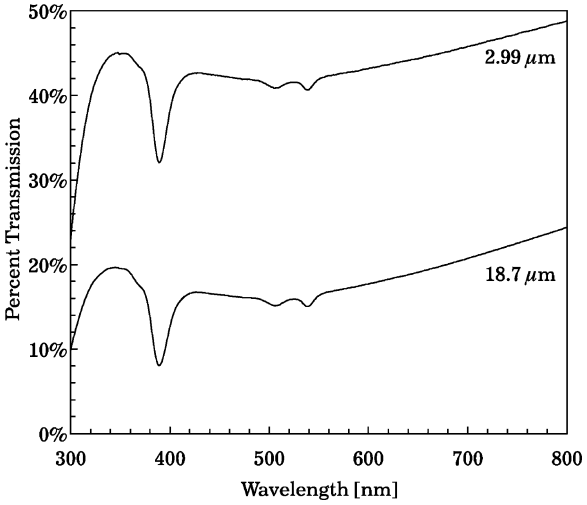

Fig. 6 Transmission spectra of PSP at two mean thicknesses.

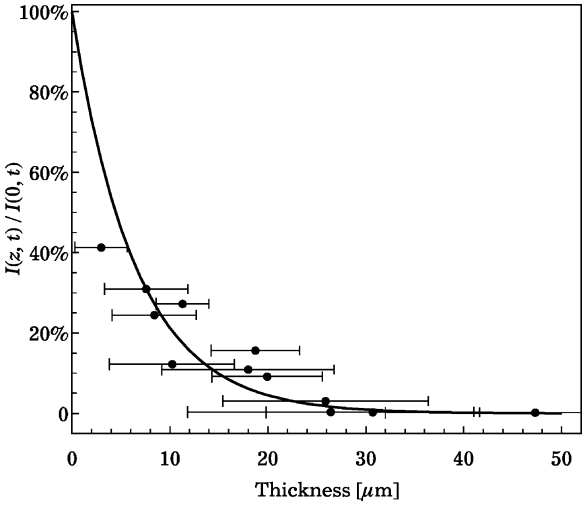

Fig. 7 Attenuation at a depth z.

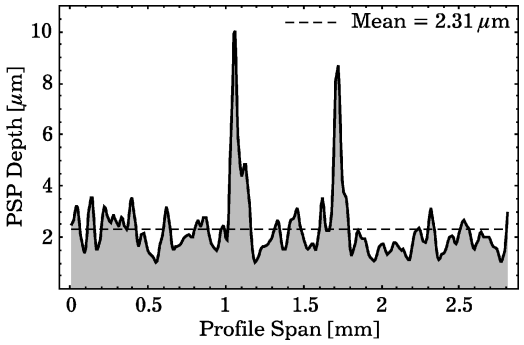

Fig. 8 Thickness profile, region 1.

Mean thickness values were calculated for each region of uniform thickness. Surface roughness values were measured as the standard deviations of thicknesses over each region. Mean paint thickness and roughness are shown in Table 1 along with the ratios of roughness to thickness (standard deviation/mean). Region 0 indicates the thickness and roughness measurement made on unpainted silicon substrate. The ratio column in Table 1 indicates that the roughness of the paint layer in region 1 is significant compared to the mean thickness, whereas the paint roughness of regions 2–5 is significantly less than the mean thickness.

Table 1 Profilometer results

Region	Thickness, μm	Roughness, μm	Thickness/ roughness
0	9.2×10^{-18}	0.02	——
1	2.3	1.4	0.60
2	7.0	1.2	0.17
3	11.5	1.6	0.14
4	24.3	2.8	0.12
5	46.3	2.2	0.047

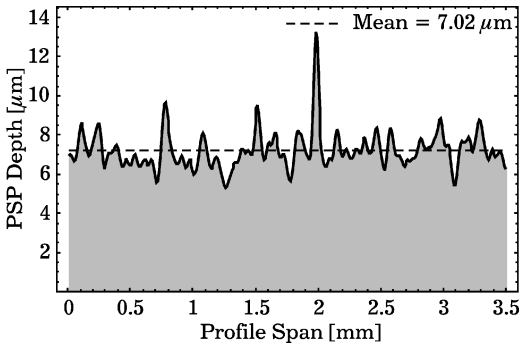

Fig. 9 Thickness profile, region 2.

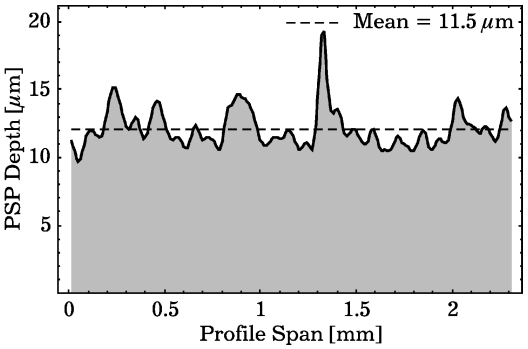

Fig. 10 Thickness profile, region 3.

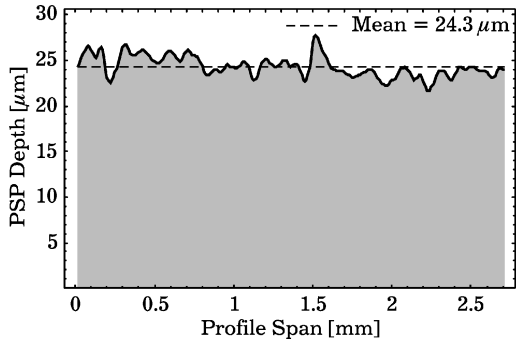

Fig. 11 Thickness profile, region 4.

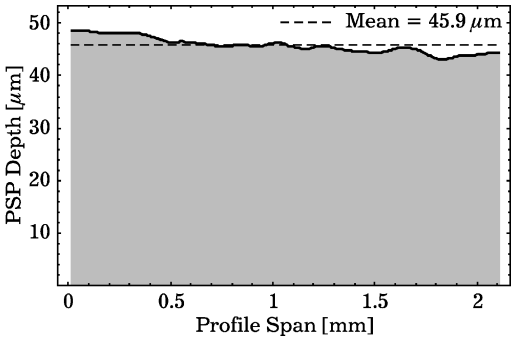

Fig. 12 Thickness profile, region 5.

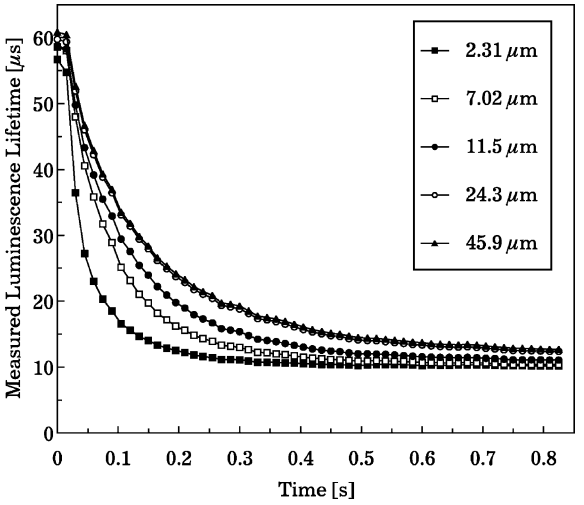

Fig. 13 Luminescence lifetime during rapid pressurization.

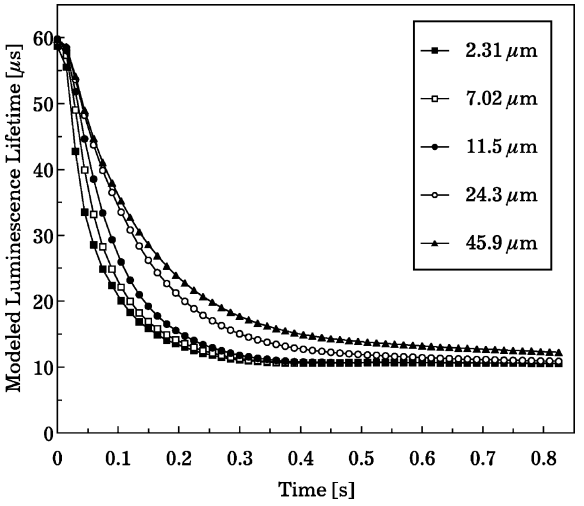

Fig. 14 Luminescence lifetimes from the mass diffusion model.

C. Lifetime Image Measurements

The sample was placed in the chamber, and the filling procedure was repeated numerous times; an excitation pulse and double-image acquisition were conducted at a different time t_p relative to the solenoid valve trigger during each repetition. Luminescence decay lifetime values τ were calculated from background-subtracted image pairs on a per-pixel basis, then averaged over regions of uniform thickness.

Pressure and luminescence lifetime data were acquired at nonuniform time steps. The finite difference scheme used to generate a solution to the mass diffusion equation requires boundary (pressure) data at uniform time increments. Therefore, $(t, P, \mathrm{d}P/\mathrm{d}t)$ data were used to interpolate a quadratic spline function, which was then sampled at uniform increments for comparison. Similarly, a linear spline function was interpolated from the nonuniform (t, τ) data, then sampled to produce uniformly sampled luminescence lifetime data. The uniformly spaced luminescence time constants are plotted in Fig. 13.

A corresponding family of luminescence lifetime curves was calculated from the mass diffusion model, and they are plotted in Fig. 14. There is an important experimental detail that must be discussed here. The paint used in this work is embedded with TiO_2 particles, to scatter the incident light and thus enhance absorption of the laser beam. This means that some laser radiation is multiply

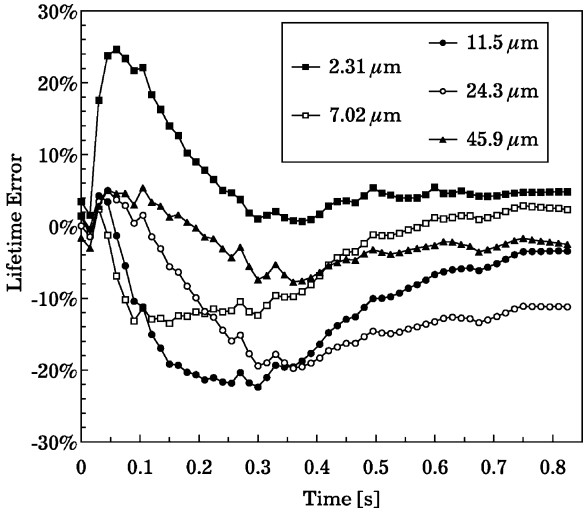

Fig. 15 Error between modeled and measured luminescence lifetime data.

scattered within the paint layer before it is absorbed. The form of Beer's law presented in Eq. (9), however, is intentionally written in a general form. The parameter κ_v is an attenuation coefficient that can represent both absorption and attenuation by multiple scattering. Here, we have measured the attenuation coefficient, and the measurement contains contributions from both processes.

The model presented here is in one spatial dimension, and that is appropriate. Multiple scattering might broaden a small excitation beam, but in this case the experiment was truly one-dimensional because the sample is uniformly illuminated, and calculations are averaged over a region of interest within the illumination boundaries.

The curves in Figs. 13 and 14 show that predicted and measured luminescence lifetimes are maximal and approximately equal at static vacuum, decrease as pressure increases, and approach equality as the oxygen concentration in the PSP layer approaches equilibrium. The predicted and measured lifetimes change more rapidly with thinner paint, whereas the response of luminescence with the thicker PSP is more gradual.

The discrepancy between the predicted and measured lifetime curves is plotted in Fig. 15 and was calculated by

$$\text{error} = (\tau_{\text{predicted}} - \tau_{\text{measured}})/\tau_{\text{measured}} \tag{18}$$

The agreement between predicted and measured lifetimes can generally be said to improve with thickness. The curves in Fig. 15 are interpreted as follows: a positive error occurs when the predicted decay lifetime is greater than the measured lifetime, that is, when measurements indicate more oxygen quenching and thus a faster response to a rapid pressure increase than was predicted by the model. Conversely, a negative difference suggests the observed quenching rate was slower than what the model predicted.

For each thickness, the discrepancy between modeled and measured response was greatest during the steepest region of the pressure change; the differences started near zero and approached zero again as the oxygen concentration approached equilibrium. The most significant error was observed with the thinnest paint, which consistently responded faster than model predictions. This is because of the high-roughness/mean-thickness ratio (see Table 1); the 2.31-μm PSP sample here is more accurately modeled as a collection of discrete peaks than as a volume with a uniform surface.

D. Pressure Measurements

Pressure was calculated by applying the Stern–Volmer function to the luminescence lifetime data. Pressure data for each thickness and transducer-measured pressure are plotted in Fig. 16. Error in the PSP pressure measurements was calculated as the difference between the transducer-measured pressure and pressure acquired from PSP luminescence lifetime data and is plotted in Fig. 17.

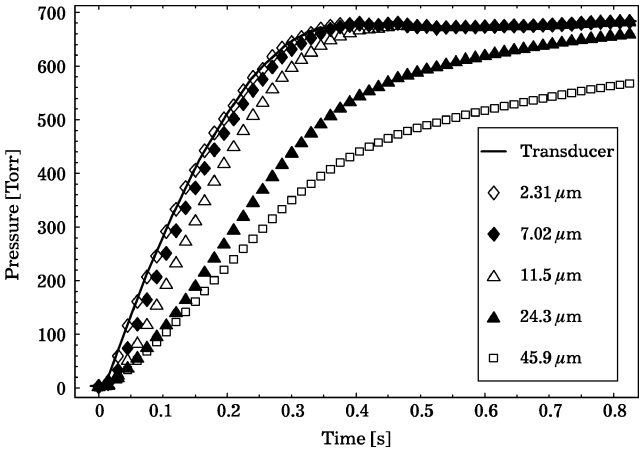

Fig. 16 Pressure calculated from luminescence lifetimes.

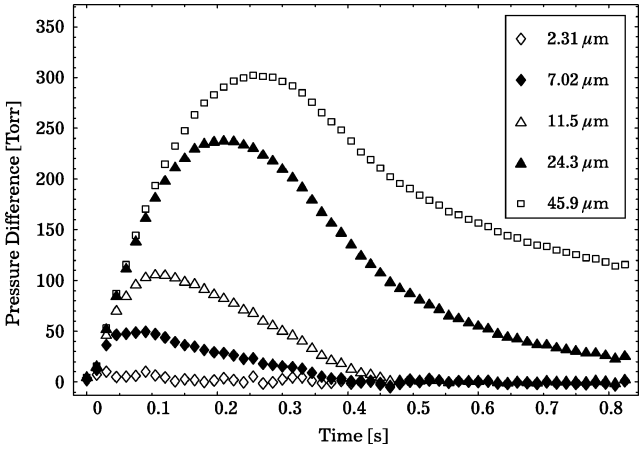

Fig. 17 Error in PSP pressure during the transient pressure function.

Figures 16 and 17 confirm that thinner PSP responds more quickly to rapidly changing pressure. After 800 ms the thicker PSP samples still had not achieved equilibrium. Conversely, the thinnest PSP layer exhibited minimal error with respect to the pressure transducer measurement.

E. Model Sensitivity to Physical Parameters

Two physical parameters embedded in Eq. (12) are the mass diffusivity constant and the optical depth. Here the effect of variations in each of these parameters on the predicted response is assessed. In each case, error was calculated as it was in Fig. 15, and rms error was calculated for each thickness. These values were tabulated as the assumed mass diffusivity constant and optical depth were singly varied.

1. Assumed Mass Diffusivity Constant

The mass diffusivity constant is a measure of the permeability of a substance (the PSP binder in this case) to mass diffusion. A higher mass diffusivity constant indicates greater permeability, that is, a layer of PSP achieves equilibrium with a changing surface pressure more efficiently with a greater mass diffusivity constant. Baron et al.[19] reported that PSP binders of increased mass diffusivity increase the response times of PSP to rapidly changing pressure. Here, the sensitivity of the irradiance emission model to variation in the assumed mass diffusivity for each thickness is plotted in Fig. 18. The data plotted in Fig. 18 were obtained as follows: the mass diffusivity constant D_m was varied from 50 to 2500 μm^2/s. For each modeled value of D_m, the luminescence lifetime was calculated over the duration of the transient pressure function for the five thicknesses of PSP. Luminescence lifetime error was calculated from each luminescence lifetime value, and each luminescence lifetime error-vs-time

Table 2 RMS error values for indicated PSP thicknesses using measured and infinite optical depths

Thickness, μm	RMS error $1/\kappa_v \to 0$ μm, %	RMS error $1/\kappa_v = 6.48$ μm, %	RMS error $1/\kappa_v \to \infty$, %
2.31	8.66	9.35	8.70
7.02	10.8	7.47	7.63
11.5	19.4	13.3	12.9
24.3	28.7	13.1	14.2
45.9	28.8	3.99	67.5

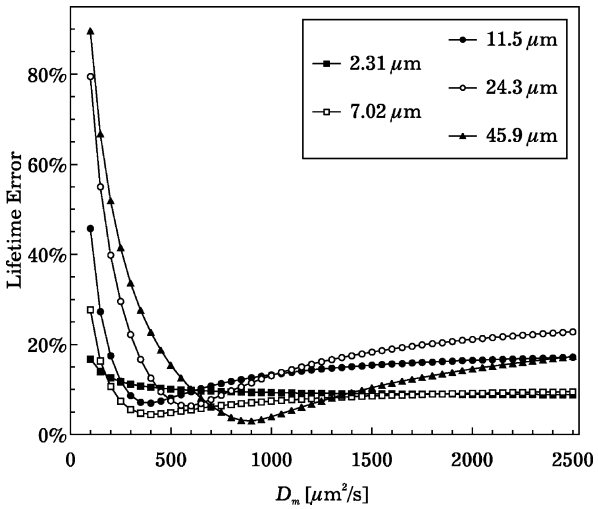

Fig. 18 RMS error as mass diffusivity was varied.

data set was reduced to a rms value. The rms lifetime error values were tabulated with mass diffusivity and plotted in Fig. 18.

The values of D_m that give the lowest lifetime error seem to increase with PSP thickness. This perception stems from the fact that the effects of mass diffusion, and therefore the uncertainty caused by an erroneous mass diffusivity constant, are only apparent as oxygen is diffusing through the PSP layer. Thinner PSP layers achieve steady-state oxygen concentrations more rapidly than thicker layers, and accordingly the rms luminescence lifetime error (calculated from lifetime data over the duration of the transient pressure function) tends to be smaller.

Except for the 2.31-μm paint, each thickness indicated a nominal mass diffusivity constant (minimum error) between ~300 and ~1000 μm^2/s. In comparison, Winslow et al. report mass diffusivities varying from 422 to 837 μm^2/s for a proprietary PSP consisting of a ruthenium-based lumiphore embedded in a silicone polymer binder.[20]

2. Optical Depth

Optical depth is the $1/\kappa_v$ term in Beer's law, Eq. (8). The error vs modeled optical depth was varied and is plotted in Fig. 19. In addition to the range of optical depths shown in Fig. 19, a value of $1/\kappa_v \to \infty$ is also of interest because this corresponds to a case of no optical attenuation, which is a common approximation in related publications. An error-vs-time plot similar to Fig. 15 is shown in Fig. 20, where $1/\kappa_v \to \infty$ was used in the model. RMS error values are shown for comparison in Table 2.

Figures 19 and 20 and Table 2 show that as $1/\kappa_v$ decreases to 0 the error grows uniformly with thickness, and as $1/\kappa_v$ increases to infinity only the thickest PSP layer shows significant error. Note too that the minimum lifetime error for 45.9-μm sample occurs when the predicted optical depth is ~7 μm; this is within ~8% of the measured optical depth (6.48 μm) obtained by the transmission experiment.

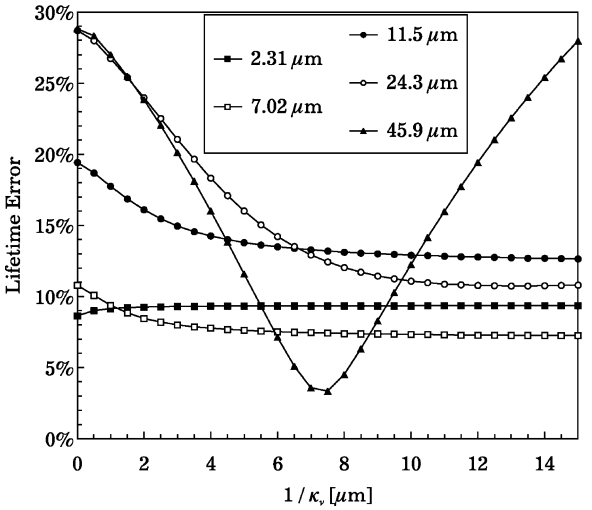

Fig. 19 RMS error as optical depth was varied.

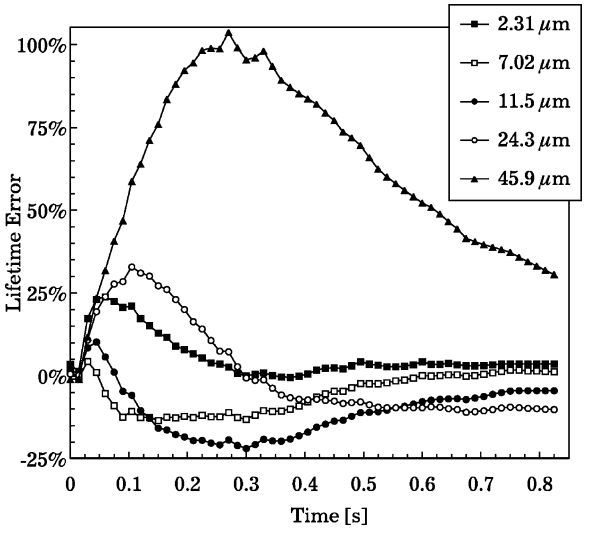

Fig. 20 Error between modeled and measured luminescence lifetime data assuming no irradiance attenuation.

VI. Conclusions

The luminescence lifetime technique has been demonstrated under unsteady pressure conditions. Although the benefits of the lifetime technique over the radiometric technique are well documented under quasi-static-pressure conditions, we have shown that the dual-image lifetime technique is well suited to an instantaneous pressure measurement during a rapid change in pressure.

A finite difference solution to the mass diffusion equation was used to model the oxygen concentration in a layer of PSP during a rapid pressure change. The oxygen concentration and optical attenuation of excitation light were then used to produce a model of the total emission response to an excitation pulse. An experiment was conducted to compare PSP lifetime measurement results to model predictions. The benefit of solving the mass diffusion equation by a numerical scheme is that unsteady pressure fields rarely follow a simple analytical form.

The comparison of measured and predicted responses during a rapid pressure change confirms previous conclusions that thin PSP coatings respond more quickly to rapidly changing pressure than thicker layers.

The results here suggest that irradiance attenuation is mildly significant for modeling the luminescence emission of thin PSP coatings, but becomes substantial for thicker coatings (~45 μm). Similarly, variations in the mass diffusivity constant used in a model do not significantly alter the predicted response for thin PSP, but

for thicker PSP the predicted mass diffusivity contributes more significantly.

Acknowledgments

The authors acknowledge support from International Scientific Solutions, Inc., and the Air Force Research Laboratory at Wright–Patterson Air Force Base under Contract F33615-96-C-2632. Roper Scientific/Princeton Instruments, Inc., was very supportive in providing digital imaging equipment and software. The authors also thank Larry P. Goss and Darryl Trump of Innovative Scientific Solutions, Inc., and Timothy R. Ohno of the Colorado School of Mines for contributions to this work.

References

[1]Demas, J. N., DeGraff, B. A., and Coleman, P. B., "Oxygen Sensors Based on Luminescence Quenching," *Analytical Chemistry*, Vol. 71, No. 23, 1999, pp. 793A–800A.

[2]Gouterman, M., "Oxygen Quenching of Luminescence of Pressure Sensitive Paint for Wind Tunnel Research," *Journal of Chemical Education*, Vol. 74, No. 6, 1997, pp. 697–702.

[3]Jules, K., Carbonaro, M., and Zemsch, S., "Application of Pressure-Sensitive Paint in Hypersonic Flows," NASA TM 106824, Feb. 1995.

[4]McLachlan, B. G., and Bell, J. H., "Pressure-Sensitive Paint in Aerodynamic Testing," *Experimental Thermal and Fluid Science*, Vol. 10, No. 4, 1995, pp. 470–485.

[5]Crites, R. C., "Pressure Sensitive Paint Technique," *VKI, Measurement Technology*, von Kármán Inst. for Fluid Dynamics, Rhode Saint Genese, Belgium, 1993, pp. 1–69.

[6]McLachlan, B. G., Kavandi, J. L., Callis, J. B., Gouterman, M., Green, E., Khalil, G., and Burns, D., "Surface Pressure Field Mapping Using Luminescent Coatings," *Experiments in Fluids*, Vol. 14, No. 1, 1993, pp. 33–41.

[7]Engler, R. H., Klein, C., and Trinks, O., "Pressure Sensitive Paint Systems for Pressure Distribution Measurements in Wind Tunnels and Turbomachines," *Measurement Science and Technology*, Vol. 11, No. 7, 2000, pp. 1077–1085.

[8]Coyle, L. M., and Gouterman, M., "Correcting Lifetime Measurements for Temperature," *Sensors and Actuators B: Chemical*, Vol. 61, No. 1, 1999, pp. 92–99.

[9]Lakowicz, J. R., Szmacinski, H., Kazimierz, N., Berndt, K. W., and Johnson, M., "Fluorescence Lifetime Imaging," *Analytical Biochemistry*, Vol. 202, 1992, pp. 316–330.

[10]Holmes, J. W., "Analysis of Radiometric, Lifetime and Fluorescent Lifetime Imaging for Pressure Sensitive Paint," *Aeronautical Journal*, Vol. 102, April 1998, pp. 189–194.

[11]Goss, L. P., Trump, D. D., Sarka, B., Lydick, L. N., and Baker, W. M., "Multi-Dimensional Time-Resolved Pressure-Sensitive-Paint Techniques—A Numerical and Experimental Comparison," AIAA Paper 2000-0832, Jan. 2000.

[12]Drouillard, T. F., II, Linne, M. A., Goss, L. P., Gord, J. R., and Fiechtner, G. J., "Lifetime Measurement and Calibration from Pressure-Sensitive Paint Luminescence Images," *Review of Scientific Instruments*, Vol. 74, No. 1, 2003, pp. 276–278.

[13]Liu, T., Guille, M., and Sullivan, J. P., "Accuracy of Pressure-Sensitive Paint," *AIAA Journal*, Vol. 39, No. 1, 2001, pp. 103–112.

[14]Oglesby, D. M., Chith, K. P., and Upchurch, B. T., "Optimization of Measurements with Pressure Sensitive Paints," NASA TM 4695, June 1995.

[15]Sajben, M., "Uncertainty Estimates for Pressure Sensitive Paint Measurements," *AIAA Journal*, Vol. 31, No. 11, 1993, pp. 2105–2110.

[16]Carroll, B., Abbitt, J., Lukas, E., and Morris, M., "Step Response of Pressure Sensitive Paints," *AIAA Journal*, Vol. 34, No. 3, 1996, pp. 521–526.

[17]Hubner, J. P., Carroll, B. F., and Ji, H. F., "Pressure-Sensitive Paint Measurements in a Shock Tube," *Experiments in Fluids*, Vol. 28, No. 1, 2000, pp. 21–28.

[18]Schairer, E. T., "Optimum Thickness of Pressure-Sensitive Paint for Unsteady Measurements," *AIAA Journal*, Vol. 40, No. 11, 2002, pp. 2312–2318.

[19]Baron, A., Danielson, D., Gouterman, M., Wan, J., Callis, J., and McLachlan, B., "Submillisecond Response Times of Oxygen Quenched Luminescent Coatings," *Review of Scientific Instruments*, Vol. 64, No. 12, 1993, pp. 3394–3402.

[20]Winslow, N. A., Carroll, B. F., and Setzer, F. M., "Frequency Response of Pressure Sensitive Paints," AIAA Paper 96-1967, June 1996.

[21]Winslow, N. A., Carroll, B. F., and Kurdila, A. J., "Model Development and Analysis of the Dynamics of Pressure-Sensitive Paints," *AIAA Journal*, Vol. 39, No. 4, 2001, pp. 660–666.

[22]Linne, M. A., *Spectroscopic Measurement: An Introduction to the Fundamentals*, Academic Press, London, 2002, Chap. 3.

[23]Drouillard, T. F., "Development of Nonintrusive Flow Field Imaging Diagnostics," Ph.D. Dissertation, Div. of Engineering, Colorado School of Mines, Golden, CO, Dec. 2002.

J. Gore
Associate Editor